Energy Correlation Coefficient in Wirelessly Powered Networks with Energy Beamforming

Na Deng
School of Information & Communication Engineering
Dalian University of Technology
Dalian, Liaoning, 116024, China
Email:dengna@dlut.edu.cn

Martin Haenggi
Dept. of Electrical Engineering
University of Notre Dame
Notre Dame, IN, 46556, USA
Email:mhaenggi@nd.edu

***Abstract*—The spatial correlation of the energy harvested from RF transmitters, named *energy correlation*, plays a key role in the performance evaluation of wirelessly powered networks. This paper introduces an analytical framework with foundations in stochastic geometry to characterize the energy correlation based on the *energy correlation coefficient* (ECC). For a model where RF power sources are distributed according to a Poisson point process and employ beamforming techniques to transfer energy directionally, we focus on two cases: i) each power source points the beam in a random direction; ii) each power source points the beam to an RF-powered node located in its Voronoi cell. We first analyze the ECC of the two cases, and then give the asymptotic results with respect to the antenna array size. It turns out that in both cases the harvested energy at two locations exhibit positive correlation, and when the antenna array size tends to infinity, the correlation in the first case vanishes while the one in the second case is still positive. Numerical results give useful insights into the effect of several system parameters on the energy correlation from directed wireless energy transfer.**

I. Introduction

Charging mobile devices wirelessly is one of the most desirable features to realize self-sustainable wireless communication networks, especially for the Internet of Things [1]. However, the harvested energy may not be enough for the information transmission due to the severe propagation loss in wireless medium. To improve wireless energy transfer (WET) efficiency, energy beamforming has been advocated in recent research [2], i.e., RF power sources are equipped with antenna arrays to form directional energy transfer beams towards devices. Although the integration of RF-based energy harvesting with beamforming technique may bring about huge benefits, it complicates the WET system and hence triggers new problems and challenges.

Clearly, performance evaluation of the directed WET is one of the most fundamental issues in wirelessly powered networks under different energy transfer policies, and the quantification of the harvested energy strongly depends on the spatial distribution of RF power sources. Since stochastic geometry has been widely used to model and analyze large-scale wireless networks, it naturally becomes a popular tool in the WET field. Regardless of the kind of wireless network being powered, the main idea behind the majority of existing works is to model the locations of both the RF sources and RF-powered nodes as independent homogeneous Poisson point processes, and investigate the average energy transfer success probability (or, equivalently, the energized probability of RF-powered nodes). Then, the energized RF-powered nodes, namely the active transmitters in the communication phase, are simply assumed to be formed by independently thinning the Poisson distributed RF-powered nodes with the energized probability [3–6]. While such analytical method leads to tractable results, the analytical insights provided are quite limited since it does not take the *energy correlation*, i.e., the spatial correlation of the energy harvested from RF transmitters, into account. This correlation, however, plays a critical role in accurately characterizing the spatial configuration of the active transmitters in the communication phase which will significantly affect the performance of wirelessly powered networks [7, 8].

In this paper, we study the spatial correlation of the energy harvested from a Poisson field of RF power sources through directional energy transfer techniques. Due to the integration of energy beamforming, the energy correlation becomes significantly more challenging than that in omni-directional WET scenario, and accordingly, the pair correlation function which is by far the most commonly used measure to characterize the spatial correlation in stochastic geometry seems infeasible. Instead, we establish an analytical framework to characterize the energy correlation through the *energy correlation coefficient* (ECC). To be specific, two energy beamforming policies are considered: one is that each RF power source randomly selects the energy beam direction; the other is that each RF-powered node harvests the energy from the aligned beam of its nearest RF power source. Using stochastic geometry, we provide analytical expressions of the ECC for the two policies. It is revealed that the energy correlation is positive in both policies and weaken in multipath. Furthermore, we give asymptotic expressions for the ECC under each policy with respect to the antenna array size. The results show that compared with omni-directional WET, the directional WET reduces the degree of the energy correlation, and different energy beamforming policies have different effects on the energy correlation. Overall, this paper provides a new analytical approach to investigate the energy correlation which does not require the specification of a point process of RF-powered nodes and captures the correlation structure directly from the energy field induced by the power sources.

II. System model

A. Network model

We consider a wireless network powered solely by ambient RF power sources (which include cellular base stations, power beacons, WiFi hotspots, etc.), where the locations of RF power sources are modeled as a Poisson point process Φ of density λ. We assume that each RF power source is equipped with a uniform linear array (ULA) composed of N antenna elements to perform directional energy beamforming, and the RF-powered node has a single antenna. The channel (power) gain between transmitter x and receiver y is given by $G_{xy}h_{xy}\ell(x-y)$, where G_{xy} is the antenna array gain determined by the energy beamforming policy, h_{xy} models the small-scale fading and $\ell(x-y)$ represents the large-scale path loss. We assume that the fading coefficient follows a gamma distribution $\mathrm{Gamma}(M, \frac{1}{M})$ (i.e., Nakagami fading), and all h_{xy} are mutually independent and also independent of the point process. We consider a bounded path loss law

$$\ell(x) = \frac{1}{\epsilon + \|x\|^{\alpha}}, \tag{1}$$

where $\epsilon > 0$ avoids having singularity at $\|x\| = 0$ and α is the path loss exponent. To maintain analytical tractability, a sectorized antenna model [9] is adopted to approximate the actual antenna pattern, and the antenna gain function is

$$G(\varphi) = \begin{cases} G_{\mathrm{m}} & \text{if } |\varphi| \le \frac{w}{2} \\ G_{\mathrm{s}} & \text{otherwise,} \end{cases} \tag{2}$$

where $\varphi \in [-\pi, \pi)$ is the angle off the beam direction, $w \in (0, 2\pi]$ is the half-power beam width, G_{m} and G_{s} are the array gains of the main and side lobes. Assuming a ULA with half-wavelength antenna spacing, we have $G_{\mathrm{m}} = N$ and $w = 4\pi G_{\mathrm{act}}^{-1}(G_{\mathrm{m}}/2)$ with $G_{\mathrm{act}}(x) = \frac{\sin^2(\pi N_{\mathrm{p}} x)}{N \sin^2(\pi x)}$ denoting the actual antenna pattern [10]. To ensure the power constraint $\frac{1}{2\pi}\int_0^{2\pi} G(\varphi)\mathrm{d}\varphi = 1$, we have $G_{\mathrm{s}} = \frac{2\pi - G_{\mathrm{m}} w}{2\pi - w}$.

B. Wireless Energy Harvesting Model

The correlation coefficient of the harvested energy at two locations is used to characterize the energy correlation caused by the specific energy beamforming policy. Due to the motion-invariance of the PPP, the correlation coefficient merely depends on the inter-point distance, i.e., the distance of two locations, and accordingly, we focus on the harvested energy at the origin o and $z = (d, 0)$. Letting $\mathcal{E}(y)$ be the harvested energy at location y, the ECC is given by

$$\chi(d) = \frac{\mathbb{E}[\mathcal{E}(o)\mathcal{E}(z)] - \mathbb{E}\mathcal{E}(o)\mathbb{E}\mathcal{E}(z)}{\sqrt{\mathrm{var}(\mathcal{E}(o))\mathrm{var}(\mathcal{E}(z))}}. \tag{3}$$

We consider two practical energy beamforming policies and establish the energy harvesting models as follows.

1) Randomly directed energy transfer (RDET) policy: In this case, each RF power source randomly selects the beam direction of the energy transfer link. Hence, for an RF-powered device located at y, its angle $\varphi_x(y)$ off the beam direction of each RF power source x is randomly and uniformly distributed in $[-\pi, \pi)$, and the antenna array gain $G(\varphi_x(y))$ has the probability mass function (PMF)

$$G(\varphi_x(y)) = \begin{cases} G_{\mathrm{m}} & \text{w.p. } q_{\mathrm{m}} = \frac{w}{2\pi} \\ G_{\mathrm{s}} & \text{w.p. } q_{\mathrm{s}} = 1 - \frac{w}{2\pi}. \end{cases} \tag{4}$$

Using the linear energy harvesting model, the harvested energy $\mathcal{E}_{\mathrm{R}}(y)$ at y from all the RF power sources is

$$\mathcal{E}_{\mathrm{R}}(y) = \sum_{x \in \Phi} G(\varphi_x(y)) h_{xy} \ell(x-y). \tag{5}$$

2) Nearest directed energy transfer (NDET) policy: In this case, each RF-powered device is associated with its nearest RF power source which aligns the beam direction pointing to one RF-powered device in its Voronoi cell[1]. Letting $x_1 \in \Phi$ be the nearest RF power source to the origin, pointing its beam to o, then the harvested energy at o is

$$\mathcal{E}_{\mathrm{N}}(o) = G_{\mathrm{m}} h_{x_1 o} \ell(x_1) + \sum_{x \in \Phi \setminus \{x_1\}} G(\varphi_x(o)) h_{xo} \ell(x). \tag{6}$$

For the harvested energy at z, we need to consider whether it has the same nearest RF power source x_1. Denote by $x_2 \in \Phi$ the nearest RF power source to z. If $x_2 = x_1$, o and z are both in the Voronoi cell of x_1. Since the time instant considered in the ECC analysis is when the origin is getting the beam targeted toward it, the harvested energy at z is

$$\begin{aligned} \mathcal{E}_{\mathrm{N}}(z) \;=\; & G(\varphi_{x_1}(z)) h_{x_1 z} \ell(x_1 - z) \\ & + \sum_{x \in \Phi \setminus \{x_1\}} G(\varphi_x(z)) h_{xz} \ell(x - z), \end{aligned} \tag{7}$$

where $G(\varphi_{x_1}(z))$ depends on the angle $\varphi_{x_1}(z)$ off the beam direction of the RF power source x_1 (namely the direction from x_1 to o). If $x_2 \neq x_1$, we focus on the case that x_2 points its beam to z and the harvested energy is

$$\mathcal{E}_{\mathrm{N}}(z) = G_{\mathrm{m}} h_{x_2 z} \ell(x_2 - z) + \sum_{x \in \Phi \setminus \{x_2\}} G(\varphi_x(z)) h_{xz} \ell(x - z). \tag{8}$$

III. Analysis of Energy Correlation Coefficient

In this section, we provide analytical results for the ECC at two locations and investigate the features of the energy correlation under RDET and NDET policies, respectively.

A. Analysis of RDET

In this policy, $\varepsilon_{\mathrm{R}}(o)$ and $\varepsilon_{\mathrm{R}}(z)$ are identically distributed but not independent, and the ECC is given by

$$\chi_{\mathrm{R}}(d) = \frac{\mathbb{E}[\mathcal{E}_{\mathrm{R}}(o)\mathcal{E}_{\mathrm{R}}(z)] - \mathbb{E}[\mathcal{E}_{\mathrm{R}}(o)]^2}{\mathbb{E}[\mathcal{E}_{\mathrm{R}}(o)^2] - \mathbb{E}[\mathcal{E}_{\mathrm{R}}(o)]^2}. \tag{9}$$

Although each RF power source randomly selects the beam direction, the antenna array gains from an RF power source to two different locations are still correlated with each other, which affects the calculation of $\mathbb{E}[\mathcal{E}_{\mathrm{R}}(o)\mathcal{E}_{\mathrm{R}}(z)]$. As a result, we first give the PMF of $\widetilde{G}(x, z) = G(\varphi_x(o))G(\varphi_x(z))$ for an RF power source x in the following lemma.

[1]If multiple (at least two) RF-powered devices have the same nearest RF power source, the beam direction could be pointed to different devices in a time-division manner.

Lemma 1. *Given that an RF power source is located at $x = (r\cos\theta, r\sin\theta)$, the PMF of $\widetilde{G}(x,z)$ is given by*

$$\widetilde{G}(x,z) = \begin{cases} G_{\rm m}^2 & \text{w.p. } \frac{w-\min(w,\nu)}{2\pi} \\ G_{\rm m}G_{\rm s} & \text{w.p. } \frac{\min(w,\nu)}{\pi} \\ G_{\rm s}^2 & \text{w.p. } 1-\frac{w+\min(w,\nu)}{2\pi}. \end{cases} \tag{10}$$

where $\nu = \arccos\left(\frac{r-d\cos\theta}{\sqrt{r^2+d^2-2rd\cos\theta}}\right)$ denotes the angle between the directions from x to o and z.

Proof: See Appendix A.

With the help of Lemma 1, we further give the ECC in the RDET case in the following theorem.

Theorem 1. *Letting $\zeta(x,z) = \mathbb{E}(\widetilde{G}(x,z))$, the ECC of $\mathcal{E}_{\rm R}(o)$ and $\mathcal{E}_{\rm R}(z)$ with the RDET policy is given by*

$$\chi_{\rm R}(d) = \frac{M}{M+1}\frac{\int_{\mathbb{R}^2}\zeta(x,z)\ell(x)\ell(x-z){\rm d}x}{(G_{\rm m}^2q_{\rm m}+G_{\rm s}^2q_{\rm s})\int_{\mathbb{R}^2}\ell^2(x){\rm d}x}. \tag{11}$$

Proof: To derive the energy correlation coefficient $\chi_{\rm R}(z)$, $\mathbb{E}\mathcal{E}_{\rm R}(o)$, $\mathbb{E}[\mathcal{E}_{\rm R}(o)^2]$ and $\mathbb{E}[\mathcal{E}_{\rm R}(o)\mathcal{E}_{\rm R}(z)]$ are needed. Firstly, using the Campbell's theorem and $\mathbb{E}h_{xo}=1$, we have

$$\mathbb{E}\mathcal{E}_{\rm R}(o) = \lambda\int_{\mathbb{R}^2}\mathbb{E}[G(\varphi_x(o))]\ell(x){\rm d}x \overset{(a)}{=} \lambda\int_{\mathbb{R}^2}\ell(x){\rm d}x, \tag{12}$$

where step (a) uses the constraint $G_{\rm m}w + G_{\rm s}(2\pi-w) = 2\pi$.

Secondly, the second moment of the harvested energy is

$$\begin{aligned}
&\mathbb{E}[\mathcal{E}_{\rm R}(o)^2] \\
&= \mathbb{E}\sum_{x\in\Phi}G^2(\varphi_x(o))h_{xo}^2\ell^2(x) \\
&\quad + \mathbb{E}\sum_{x,y\in\Phi}^{x\neq y}G(\varphi_x(o))G(\varphi_y(o))h_{xo}h_{yo}\ell(x)\ell(y) \\
&\overset{(b)}{=} \lambda\frac{M+1}{M}\int_{\mathbb{R}^2}\mathbb{E}[G^2(\varphi_x(o))]\ell^2(x){\rm d}x \\
&\quad + \lambda^2\int_{\mathbb{R}^2}\int_{\mathbb{R}^2}\mathbb{E}[G(\varphi_x(o))]\ell(x)\mathbb{E}[G(\varphi_y(o))]\ell(y){\rm d}x{\rm d}y \\
&= \lambda\frac{(G_{\rm m}^2q_{\rm m}+G_{\rm s}^2q_{\rm s})(M+1)}{M}\int_{\mathbb{R}^2}\ell^2(x){\rm d}x + \mathbb{E}[\mathcal{E}_{\rm R}(o)]^2,
\end{aligned} \tag{13}$$

where step (b) follows from the independence of h_{xo} and h_{yo}, $\mathbb{E}[h_{xy}^2] = (M+1)/M$, the independence of $G(\varphi_x(o))$ and $G(\varphi_y(o)))$ as well as the second-order product density formula of the PPP [11].

Lastly, the mean of $\mathcal{E}_{\rm R}(o)\mathcal{E}_{\rm R}(z)$ is

$$\begin{aligned}
&\mathbb{E}[\mathcal{E}_{\rm R}(o)\mathcal{E}_{\rm R}(z)] \\
&= \mathbb{E}\sum_{x\in\Phi}G(\varphi_x(o))G(\varphi_x(z))h_{xo}\ell(x)h_{xz}\ell(x-z) \\
&\quad + \mathbb{E}\sum_{x,y\in\Phi}^{x\neq y}G(\varphi_x(o))G(\varphi_y(z))h_{xo}h_{yz}\ell(x)\ell(y-z) \\
&\overset{(c)}{=} \lambda\int_{\mathbb{R}^2}\mathbb{E}[\widetilde{G}(x,z)]\ell(x)\ell(x-z){\rm d}x \\
&\quad + \lambda^2\int_{\mathbb{R}^2}\int_{\mathbb{R}^2}\mathbb{E}[G(\varphi_x(o))]\ell(x)\mathbb{E}[G(\varphi_y(z))]\ell(y-z){\rm d}x{\rm d}y \\
&= \lambda\int_{\mathbb{R}^2}\zeta(x,z)\ell(x)\ell(x-z){\rm d}x + \mathbb{E}[\mathcal{E}_{\rm R}(o)]^2,
\end{aligned} \tag{14}$$

where step (c) follows by similar reasoning as step (b). ∎

From (11), we observe that the ECC is positive and increases with the fading parameter M. Put differently, the small-scale fading (especially in multipath) reduces the energy correlation under the RDET policy. Moreover, it is interesting to explore how the antenna array size N (or, equivalently, the beamwidth) affects the correlation and what happens when $N\to\infty$.

Corollary 1. *Letting $N\to\infty$, we have $\chi_{\rm R}(d)\to 0$.*

Proof: When $N\to\infty$, we have $G_{\rm m}\to\infty$ and $w\to 0$. Furthermore, according to the power constraint, we have $G_{\rm s} < 1$. Thus, it is obtained that

$$\widetilde{G}(x,z) = \begin{cases} G_{\rm m}G_{\rm s} & \text{w.p. } \frac{w}{\pi} \\ G_{\rm s}^2 & \text{w.p. } 1-\frac{w}{\pi}, \end{cases} \tag{15}$$

and

$$\zeta(x,z) = \frac{w}{\pi}G_{\rm m}G_{\rm s} + (1-\frac{w}{\pi})G_{\rm s}^2. \tag{16}$$

Then, the energy correlation coefficient can be further expressed as

$$\begin{aligned}
\chi_{\rm R}(d) &= \frac{G_{\rm m}G_{\rm s}\frac{w}{\pi}+G_{\rm s}^2(1-\frac{w}{\pi})}{G_{\rm m}^2\frac{w}{2\pi}+G_{\rm s}^2(1-\frac{w}{2\pi})}\underbrace{\frac{M\int_{\mathbb{R}^2}\ell(x)\ell(x-z){\rm d}x}{(M+1)\int_{\mathbb{R}^2}\ell^2(x){\rm d}x}}_{\mathcal{A}} \\
&= \mathcal{A}\frac{2wG_{\rm s}+G_{\rm s}^2(\pi-w)/G_{\rm m}}{G_{\rm m}w+G_{\rm s}(2\pi-w)+(\frac{G_{\rm s}^2}{G_{\rm m}}-G_{\rm s})(2\pi-w)} \\
&= \mathcal{A}\frac{2wG_{\rm s}+G_{\rm s}^2(\pi-w)/G_{\rm m}}{2\pi+(\frac{G_{\rm s}^2}{G_{\rm m}}-G_{\rm s})(2\pi-w)} \to 0.
\end{aligned} \tag{17}$$

∎

Remark 1. *This corollary shows that the energy correlation at two locations becomes uncorrelated when $N\to\infty$, which implies that using the independent thinning method to form the energized RF-powered devices is only accurate in the extreme case when the RF power sources are equipped with infinite antenna arrays.*

B. Analysis of NDET

In this policy, each RF power source points the beam to the powered devices lying in its Voronoi region. As a consequence, it is possible that two RF-powered nodes have the same nearest RF power source, which significantly complicates the theoretical derivations. To simplify it, the total harvested energy from all RF power sources is approximated by the harvested energy from the nearest RF power source, resulting in $\mathcal{E}_{\rm N}(o) \approx G_{\rm m}h_{x_1o}\ell(x_1)$ and

$$\mathcal{E}_{\rm N}(z) \approx \begin{cases} G(\varphi_{x_1}(z))h_{x_1z}\ell(x_1-z) & \text{if } x_2 = x_1 \\ G_{\rm m}h_{x_2z}\ell(x_2-z) & \text{if } x_2\neq x_1. \end{cases} \tag{18}$$

To characterize the energy correlation, it is necessary to derive the distance distribution of $R_2 = \|x_2 - z\|$, which is given in the following lemma. For notational convenience, we define $R \triangleq \sqrt{r^2+d^2-2rd\cos\theta}$, and

$$A(r_1,r_2,d) \triangleq \begin{cases} \pi(\min\{r_1,r_2\})^2, & d \le |r_1-r_2| \\ r_1^2\varphi_1 + r_2^2\varphi_2 - s_\Delta, & |r_1-r_2| < d < r_1+r_2 \\ 0, & \text{otherwise} \end{cases} \quad (19)$$

is the intersection area of two disks with radii r_1 and r_2 at distance d, where

$$\varphi_1 = \arccos\left(\frac{r_1^2+d^2-r_2^2}{2r_1 d}\right), \quad (20)$$

$$\varphi_2 = \arccos\left(\frac{r_2^2+d^2-r_1^2}{2r_2 d}\right), \quad (21)$$

$$s_\Delta = \frac{1}{2}\sqrt{[(r_1+r_2)^2-d^2][d^2-(r_1-r_2)^2]}. \quad (22)$$

Lemma 2. *Given that the nearest RF power source to the origin x_1 is located at $(r\cos\theta, r\sin\theta)$, the two locations z and o have the same nearest RF power source with probability*

$$\varpi(r,\theta) = e^{-\lambda(\pi R^2 - A(R,r,d))}, \quad (23)$$

and the unconditional probability is

$$p_{\text{same}} = \int_0^\pi \int_0^\infty 2\lambda r e^{-\lambda\pi r^2}\varpi(r,\theta)\mathrm{d}r\mathrm{d}\theta. \quad (24)$$

Conditioned on $x_2 \neq x_1$, the cumulative distribution function of the distance R_2 is given by

$$F_{R_2}(r_2) = \begin{cases} \frac{1-e^{-\lambda(\pi r_2^2 - A(r_2,r,d))}}{1-\varpi(r,\theta)} & r_2 \in [\psi(r), R] \\ 0 & \textit{otherwise}. \end{cases} \quad (25)$$

where $\psi(r) = \max(0, r-d)$.

Proof: See Appendix B.

Theorem 2. *The ECC of $\mathcal{E}_{\mathrm{N}}(o)$ and $\mathcal{E}_{\mathrm{N}}(z)$ with the NDET policy is approximated as*

$$\chi_{\mathrm{N}}(d) \approx \frac{\xi_{zo} - \eta_o\eta_z}{\sqrt{(\kappa_o - \eta_o^2)(\kappa_z - \eta_z^2)}}, \quad (26)$$

where

$$\eta_o = \pi\lambda\int_0^\infty \frac{e^{-\pi\lambda r}}{\epsilon + r^{\alpha/2}}\mathrm{d}r, \quad (27)$$

$$\kappa_o = \pi\lambda\frac{M+1}{M}\int_0^\infty \frac{e^{-\pi\lambda r}}{(\epsilon + r^{\alpha/2})^2}\mathrm{d}r, \quad (28)$$

$$\eta_z = \int_0^\pi\int_0^\infty 2\lambda r e^{-\pi\lambda r^2}\left[\frac{\varpi(r,\theta)G(r,\theta)}{\epsilon + R^\alpha} + \int_{\psi(r)}^R (1-\varpi(r,\theta))\frac{\mathrm{d}F_{R_2}(r_2)}{\epsilon + r_2^\alpha}\right]\mathrm{d}r\mathrm{d}\theta, \quad (29)$$

$$\kappa_z = \frac{M+1}{M}\int_0^\pi\int_0^\infty 2\lambda r e^{-\pi\lambda r^2}\left[\frac{\varpi(r,\theta)G^2(r,\theta)}{(\epsilon + R^\alpha)^2} + \int_{\psi(r)}^R (1-\varpi(r,\theta))\frac{\mathrm{d}F_{R_2}(r_2)}{(\epsilon + r_2^\alpha)^2}\right]\mathrm{d}r\mathrm{d}\theta, \quad (30)$$

$$\xi_{zo} = \int_0^\pi\int_0^\infty 2\lambda r e^{-\pi\lambda r^2}\left[\frac{\varpi(r,\theta)G(r,\theta)}{(\epsilon + r^\alpha)(\epsilon + R^\alpha)} + \int_{\psi(r)}^R (1-\varpi(r,\theta))\frac{\mathrm{d}F_{R_2}(r_2)}{(\epsilon + r^\alpha)(\epsilon + r_2^\alpha)}\right]\mathrm{d}r\mathrm{d}\theta, \quad (31)$$

$$G(r,\theta) = \begin{cases} 1 & \textit{if } |\arccos(\frac{r-z\cos(\theta)}{R})| \le \frac{w}{2} \\ G_{\mathrm{s}}/G_{\mathrm{m}} & \textit{otherwise}. \end{cases} \quad (32)$$

Proof: Using the contact distance distribution of the PPP $f_{\|x_1\|}(r) = 2\pi\lambda r e^{-\pi\lambda r^2}$ [12], it is easy to derive the first- and second-order moments of the approximate harvested energy at the origin. For $\mathcal{E}_{\mathrm{N}}(z)$ in (18), its expectation is derived as

$$\begin{aligned} \mathbb{E}\mathcal{E}_{\mathrm{N}}(z) &= \mathbb{E}[G(\varphi_{x_1}(z))h_{x_1 z}\ell(x_1 - z) \mid x_2 = x_1] \\ &\quad + \mathbb{E}[G_{\mathrm{m}}h_{x_2 z}\ell(x_2 - z) \mid x_2 \neq x_1] \\ &\overset{(a)}{=} \int_0^{2\pi}\int_0^\infty \frac{f_{\|x_1\|}(r)}{2\pi}\frac{\varpi(r,\theta)\bar{G}(r,\theta)}{\epsilon + \|x_1 - z\|^\alpha}\mathrm{d}r\mathrm{d}\theta \\ &\quad + \int_0^{2\pi}\int_0^\infty \frac{f_{\|x_1\|}(r)}{2\pi}\mathbb{E}_{x_2}\Big[\frac{(1-\varpi(r,\theta))G_{\mathrm{m}}}{\epsilon + \|x_2 - z\|^\alpha}\Big]\mathrm{d}r\mathrm{d}\theta \\ &\overset{(b)}{=} \int_0^{\pi}\int_0^\infty \frac{f_{\|x_1\|}(r)}{\pi}\frac{\varpi(r,\theta)\bar{G}(r,\theta)}{\epsilon + R^\alpha}\mathrm{d}r\mathrm{d}\theta \\ &\quad + \int_0^{\pi}\int_0^\infty \frac{f_{\|x_1\|}(r)}{\pi}\mathbb{E}_{R_2}\Big[\frac{(1-\varpi(r,\theta))G_{\mathrm{m}}}{\epsilon + R_2^\alpha}\Big]\mathrm{d}r\mathrm{d}\theta \\ &= \int_0^\pi\int_0^\infty 2\lambda r e^{-\pi\lambda r^2}\Bigg[\frac{\varpi(r,\theta)\bar{G}(r,\theta)}{\epsilon + R^\alpha} \\ &\quad + \int_{\psi(r)}^R (1-\varpi(r,\theta))\frac{G_{\mathrm{m}}\mathrm{d}F_{R_2}(r_2)}{\epsilon + r_2^\alpha}\Bigg]\mathrm{d}r\mathrm{d}\theta, \end{aligned} \quad (33)$$

where step (a) follows that the angle θ of x_1 is uniformly distributed in $[0, 2\pi)$ and $\bar{G}(r,\theta)$ is the array gain from x_1 to z when x_1 points its beam to o, given by

$$\bar{G}(r,\theta) = \begin{cases} G_{\mathrm{m}} & \text{if } |\arccos(\frac{r-z\cos(\theta)}{R})| \le \frac{w}{2} \\ G_{\mathrm{s}} & \text{otherwise.} \end{cases} \quad (34)$$

and step (b) follows from the symmetry of $\theta \in [0,\pi]$ and $[\pi, 2\pi]$ and $R_2 = \|x_2 - z\|$.

Similar to the derivation of $\mathbb{E}\mathcal{E}_{\mathrm{N}}(z)$, we can also obtain the expressions of $\mathbb{E}[\mathcal{E}_{\mathrm{N}}(z)^2]$ and $\mathbb{E}[\mathcal{E}_{\mathrm{N}}(o)\mathcal{E}_{\mathrm{N}}(z)]$. Substituting the above results into (3), the final result is obtained. ■

It is observed that increasing M reduces both κ_o and κ_z, and hence increases the ECC under the NDET policy. Furthermore, we also investigate what happens to the energy correlation when $N \to \infty$.

Corollary 2. *Letting $N \to \infty$, we have*

$$\chi_{\mathrm{N}}(d) \to \frac{\tilde{\xi}_{zo} - \eta_o\tilde{\eta}_z}{\sqrt{(\kappa_o - \eta_o^2)(\tilde{\kappa}_z - \tilde{\eta}_z^2)}}, \quad (35)$$

where

$$\tilde{\eta}_z = \int_0^\pi\int_0^\infty\int_{\psi(r)}^R 2\lambda r e^{-\pi\lambda r^2}\frac{(1-\varpi(r,\theta))\mathrm{d}F_{R_2}(r_2)}{\epsilon + r_2^\alpha}\mathrm{d}r\mathrm{d}\theta,$$

$$\tilde{\kappa}_z = \frac{2\lambda(M+1)}{M}\int_0^\pi\int_0^\infty\int_{\psi(r)}^R \frac{r e^{-\pi\lambda r^2}(1-\varpi(r,\theta))\mathrm{d}F_{R_2}(r_2)}{(\epsilon + r_2^\alpha)^2}\mathrm{d}r\mathrm{d}\theta,$$

$$\tilde{\xi}_{zo} = \int_0^\pi\int_0^\infty\int_{\psi(r)}^R 2\lambda r e^{-\pi\lambda r^2}\frac{(1-\varpi(r,\theta))\mathrm{d}F_{R_2}(r_2)}{(\epsilon + r^\alpha)(\epsilon + r_2^\alpha)}\mathrm{d}r\mathrm{d}\theta.$$

Proof: When $N \to \infty$, we have $w \to 0$ and $G_{\mathrm{s}}/G_{\mathrm{m}} \to 0$, and the final results are obtained. ■

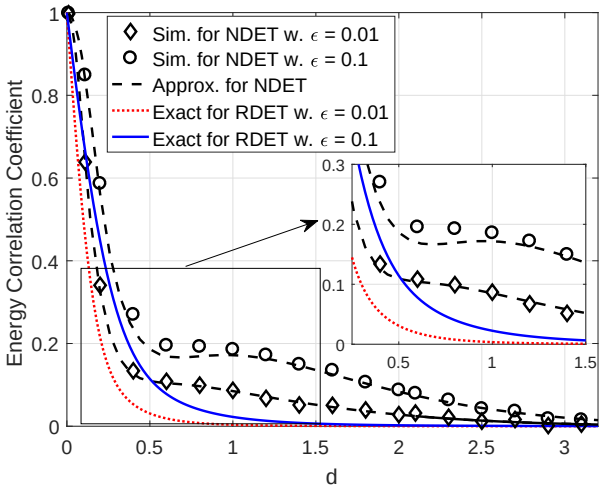

Fig. 1. The ECCs versus the inter-point distance for RDET and NDET.

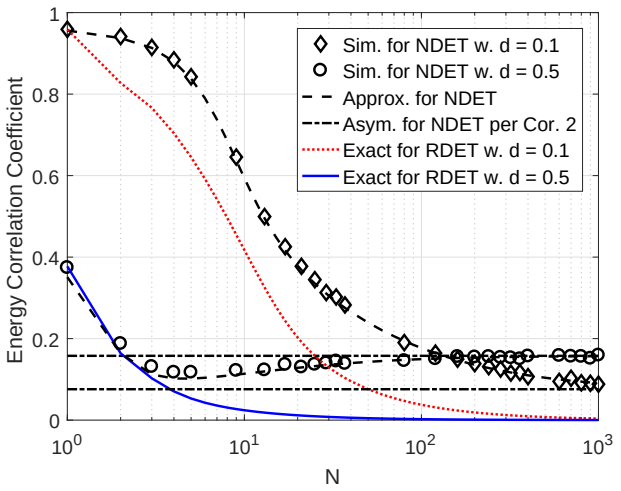

Fig. 2. The ECCs versus the antenna array size for RDET and NDET.

Remark 2. *This corollary implies that the correlation of the harvested energy at two locations does not disappear when $N \to \infty$, which means the energized point process cannot be simply approximated by independently thinning the point process of RF-powered devices.*

IV. Numerical Results

In this section, the ECCs are evaluated for the RDET and NDET policies to illustrate their relation and the effects of system parameters, where the small-scale channel fading is ignored (i.e., $M \to \infty$). The default system parameters are $\lambda = 0.1$, $\alpha = 4$, $\epsilon = 0.01$, and $N = 8$.

Fig. 1 plots the ECC as a function of the inter-point distance d with different ϵ for the RDET and NDET. It can be seen that the approximate analytical results of the NDET policy match the simulation results well, which confirms the accuracy and effectiveness of the proposed approximation. From the overall trend, the ECCs for both policies are positive and decrease with the increase of d, finally tending to zero for different parameter settings. The difference is that NDET yields a larger ECC (i.e., stronger energy correlation) and decreases to zero with a lower rate than RDET. This comes from the difference in transmitting directional beams, and the random directed policy reduces the energy correlation. Moreover, it is observed that a smaller ϵ leads to a weaker energy correlation between two locations. The reason is that the nearby RF power sources usually contribute more energy to RF-powered nodes than the others, and as ϵ decreases, their contributions become more dominant to the total energy that can be harvested.

Fig. 2 illustrates the ECC versus the antenna array size N for different inter-point distances d under the RDET and NDET policies. For the RDET policy, it is shown that the ECC decreases with the increase of N. This is because the amount of the harvested energy highly depends on the main lobe of the RF power source, and a narrower beam formed by a larger antenna array decreases the probability that two RF-powered nodes are covered by the main lobe of the same RF power source. In other words, narrowing the beamwidth decreases the energy correlation. Compared with the RDET, NDET is a more complicated case and its ECC curves are more interesting and distinctive: 1) for different d, the ECC does not always change monotonically with N; 2) each curve of the NDET converges to the extreme case of $N \to \infty$; 3) the ECC of $d = 0.1$ is higher than that of $d = 0.5$ when $N < 100$, and the opposite phenomenon occurs when $N > 100$. In the NDET policy, there are two possible cases: one is that the two RF-powered nodes have the same RF power source, with the probability of 0.96 and 0.81 for $d = 0.1$ and $d = 0.5$, respectively; and the other is that the two RF-powered nodes have different nearest RF power sources. Thus, the reason behind the above observations is that the energy correlation is dominated by the former or the latter case, which is closely related with the inter-point distance and antenna array size.

V. Conclusions

In this paper, we analyzed the ECC in a wirelessly powered network where the RF power sources are distributed according to a PPP and transfer the energy directionally through two energy beamforming policies. We proved that the energy harvested from directed RF beams are spatially correlated, which should be taken into account when analyzing the WET-enabled communication performance. Besides, we found that the introduction of the energy beamforming technique weakens the energy correlation as in the omni-directional case, and different energy beamforming policies would result in distinct features of energy correlation, which should be carefully selected according to the specific kind of RF sources and their applicable scenes. It is also shown that parameters regarding to the pathloss and small-scale fading, the inter-point distance as well as the antenna array size have significant impacts on the spatial correlated degree of the harvested energy. In the future, the ECC analysis will play an important role in the modeling of the WET-enabled communication networks and the communication performance analysis.

ACKNOWLEDGMENT

This work was supported by the National Natural Science Foundation of China under Grant 61701071, and by the US National Science Foundation under Grant 2007498.

APPENDIX A
PROOF OF LEMMA 1

Proof: As shown in the left figure of Fig. 3, ν denotes the angle between the directions from x to o and z, and according to the cosine law, we have $\nu = \arccos\left(\frac{r-d\cos\theta}{\sqrt{r^2+d^2-2rd\cos\theta}}\right)$. $\widetilde{G}(x,z)$ depends on the relative angle relationship between ν and the beam direction. We first consider the case of $\nu \geq w$ and $\widetilde{G}(x,z)$ can be either $G_{\rm s}^2$ or $G_{\rm m}G_{\rm s}$. Since the beam direction is uniformly distributed in $[0,2\pi]$, the probability of merely one direction (either $x \to z$ or $x \to o$) lying in the beam is $\frac{2w}{2\pi}$. Thus, we have

$$\widetilde{G}(x,z) = \begin{cases} G_{\rm m}G_{\rm s} & \text{w.p. } \frac{w}{\pi} \\ G_{\rm s}^2 & \text{w.p. } 1-\frac{w}{\pi}. \end{cases} \tag{36}$$

For the case of $\nu < w$, the probability of the two directions (both $x \to z$ and $x \to o$) lying in the beam is $\frac{w-\nu}{2\pi}$, and then the probability of merely one direction (either $x \to z$ or $x \to o$) lying in the beam is $\frac{2\nu}{2\pi}$. So we have

$$\widetilde{G}(x,z) = \begin{cases} G_{\rm m}^2 & \text{w.p. } \frac{w-\nu}{2\pi} \\ G_{\rm m}G_{\rm s} & \text{w.p. } \frac{\nu}{\pi} \\ G_{\rm s}^2 & \text{w.p. } 1-\frac{w+\nu}{2\pi}. \end{cases} \tag{37}$$

Combining the above two cases, the final result is obtained. ■

APPENDIX B
PROOF OF LEMMA 2

As shown in the right figure of Fig. 3, x_1 is the nearest RF power source to the origin o and R denotes the distance from x_1 to z. We first derive the probability of o and z having the same nearest RF power source x_1, which is equivalent to the case that no RF power source is in the shadow region. Then the corresponding probability of this event is given by

$$\varpi(r,\theta) = e^{-\lambda(\pi R^2 - A(R,r,d))}, \tag{38}$$

where $\pi R^2 - A(R,r,d)$ is the area of the shadow region. The unconditional probability is obtained by using the contact distance distribution of the PPP $f_{\|x_1\|}(r) = 2\pi\lambda r e^{-\pi\lambda r^2}$ [12] and the angle θ of x_1 randomly uniformly distributed in $[0,2\pi)$, and we have

$$\begin{aligned} p_{\rm same} &= \int_0^{2\pi}\int_0^{\infty} \frac{1}{2\pi} f_{\|x_1\|}(r)\varpi(r,\theta)\mathrm{d}r\mathrm{d}\theta \\ &\overset{(a)}{=} \int_0^{\pi}\int_0^{\infty} 2\lambda r e^{-\pi\lambda r^2}\varpi(r,\theta)\mathrm{d}r\mathrm{d}\theta, \end{aligned} \tag{39}$$

where step (a) follows the symmetry of $\varpi(r,\theta)$ over $\theta \in [0,\pi]$ and $[\pi,2\pi]$.

Secondly, conditioned on z having a different nearest RF power source x_2, the cumulative distribution function of the distance from x_2 to z, denoted by R_2, is given by

$$F_{R_2}(r_2) = \mathbb{P}(R_2 < r_2 \mid x_2 \neq x_1)$$

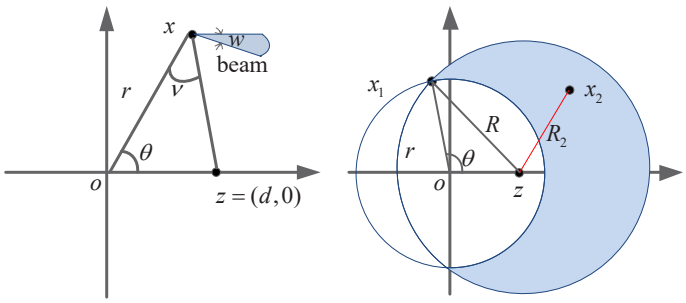

Fig. 3. Illustrations for the proofs of Lemma 1 (left) and Lemma 2 (right).

$$= \frac{\mathbb{P}(\mathcal{X})}{1-e^{-\lambda(\pi R^2 - A(R,r,d))}}, \tag{40}$$

where $\mathcal{X}$ denotes the event that there is no RF power source in the region $b(z,r_2)\setminus b(z,r_2)\cap b(o,r)$, and thus we have

$$\mathbb{P}(\mathcal{X}) = 1 - e^{-\lambda(\pi r_2^2 - A(r_2,r,d))}. \tag{41}$$

According to the geometrical relationship, we further obtain $R_2 \in [\max(0, r-d), R]$.

REFERENCES

[1] S. Bi, Y. Zeng, and R. Zhang, "Wireless powered communication networks: an overview," *IEEE Wireless Communications*, vol. 23, no. 2, pp. 10–18, April 2016.

[2] L. Liu, R. Zhang, and K. Chua, "Multi-antenna wireless powered communication with energy beamforming," *IEEE Transactions on Communications*, vol. 62, no. 12, pp. 4349–4361, 2014.

[3] K. Huang and V. K. N. Lau, "Enabling wireless power transfer in cellular networks: Architecture, modeling and deployment," *IEEE Transactions on Wireless Communications*, vol. 13, no. 2, pp. 902–912, Feb. 2014.

[4] M. Di Renzo and W. Lu, "System-level analysis and optimization of cellular networks with simultaneous wireless information and power transfer: Stochastic geometry modeling," *IEEE Transactions on Vehicular Technology*, vol. 66, no. 3, pp. 2251–2275, March 2017.

[5] L. Wang, K. Wong, R. W. Heath, and J. Yuan, "Wireless powered dense cellular networks: How many small cells do we need?" *IEEE Journal on Selected Areas in Communications*, vol. 35, no. 9, pp. 2010–2024, Sep. 2017.

[6] X. Zhou, J. Guo, S. Durrani, and M. Di Renzo, "Power beacon-assisted millimeter wave ad hoc networks," *IEEE Transactions on Communications*, vol. 66, no. 2, pp. 830–844, Feb 2018.

[7] N. Deng and M. Haenggi, "The energized point process as a model for wirelessly powered communication networks," *IEEE Transactions on Green Communications and Networking*, vol. 4, no. 3, pp. 832–844, Sept. 2020.

[8] ——, "A tractable model for wirelessly powered networks with energy correlation," *IEEE Transactions on Wireless Communications*, vol. 19, no. 9, pp. 5765–5778, Sept. 2020.

[9] S. Singh, M. N. Kulkarni, A. Ghosh, and J. G. Andrews, "Tractable model for rate in self-backhauled millimeter wave cellular networks," *IEEE Journal on Selected Areas in Communications*, vol. 33, no. 10, pp. 2196–2211, Oct. 2015.

[10] N. Deng, M. Haenggi, and Y. Sun, "Millimeter-wave device-to-device networks with heterogeneous antenna arrays," *IEEE Transactions on Communications*, vol. 66, no. 9, pp. 4271–4285, Sep. 2018.

[11] M. Haenggi, *Stochastic geometry for wireless networks*. Cambridge University Press, 2012.

[12] ——, "On distances in uniformly random networks," *IEEE Transactions on Information Theory*, vol. 51, no. 10, pp. 3584–3586, Oct. 2005.